



www.chemsuschem.org

# CsPbBr<sub>3</sub> Perovskite Nanocrystals for Photocatalytic [3+2] Cycloaddition

Yixiong Lin<sup>[a]</sup> and Yong Yan\*<sup>[a]</sup>

Visible-light-induced halide-exchange between halide perovskite and organohalide solvents has been studied in which photoinduced electron transfer from CsPbBr<sub>3</sub> nanocrystals (NCs) to dihalomethane solvent molecules produces halide anions via reductive dissociation, followed by a spontaneous anionexchange. Photogenerated holes in this process are less focused. Here, for CsPbBr<sub>3</sub> in dibromomethane (DBM), we discover that Br radical (Br\*) is a key intermediate resulting from the hole oxidation. We successfully trapped Br\* with reported methods and found that Br\* is continuously generated in DBM under visible light irradiation, hence imperative for catalytic reaction design. Continuous Br\* formation within this halide-

exchange process is active for photocatalytic [3+2] cycloaddition for vinylcyclopentane synthesis, a privileged scaffold in medicinal chemistry, with good yield and rationalized diastereoselectivity. The NC photocatalyst is highly recyclable due to Br-based self-healing, leading to a particularly economic and neat heterogeneous reaction where the solvent DBM also acts as a co-catalyst in perovskite photocatalysis. Halide perovskites, notable for efficient solar energy conversion, are demonstrated as exceptional photocatalysts for Br radical-mediated [3+2] cycloaddition. We envisage such perovskite-induced Br radical strategy may serve as a powerful chemical tool for developing valuable halogen radical-involved reactions.

## Introduction

Lead-halide perovskites have lately been shown to be an exceptional material candidate for highly efficient solar cells, [1] photodetectors, [2] LEDs, [3] lasers, [4] transistors, [5] piezoelectrics, [6] sensors, [7] as well as outstanding catalysts for renewable fuel generation<sup>[8]</sup> and photoredox organic reactions.<sup>[9]</sup> The application of lead-halide perovskite for visible-light-driven synthesis of pharmaceutically important scaffolds is continuously thriving, as demonstrated by recent examples for heterocyclization<sup>[10]</sup> and further functionalization of heterocycles.[11] One of the unique properties of such perovskites is their easily accessible band tunings in which simple halide-exchange may tune the bandgaps of perovskites that essentially span the entire visible light spectrum. [12] As shown in Scheme 1A, halide perovskite ABX<sub>3</sub> demonstrates spontaneous halide-exchange with free halogen ions in solution, i.e., CsPbBr<sub>3</sub> readily exchanged with I<sup>-</sup> ions, forming CsPbBr<sub>3-x</sub>l<sub>xr</sub> or with Cl<sup>-</sup> ions forming CsPbBr<sub>3-x</sub>Cl<sub>x</sub>.<sup>[12]</sup> Visible-light-induced halide-exchange of perovskite NCs was discovered by Parobek et al. directly between an organohalide solvent and lead-halide perovskite, i.e., CsPbBr<sub>3</sub> with dichloroA) Spontaneous perovskite halide-exchange (X = Cl, Br, I):

\_(spontaneous) CsPbBr<sub>3-x</sub>X<sub>x</sub>

B) Parobek et al.: light-induced halide-exchange between perovskite and halogen solvents

CsPbBr<sub>3</sub> + CH<sub>2</sub>Cl<sub>2</sub> 
$$\xrightarrow{h\upsilon}$$
 CsPbBr<sub>3-x</sub>Cl<sub>x</sub>

CsPbCl<sub>3</sub> + CH<sub>2</sub>Br<sub>2</sub>  $\xrightarrow{h\upsilon}$  CsPbCl<sub>3-x</sub>Br<sub>x</sub>

C) Our previous report: halide-exchange for perovskite photocatalyst activation

When X = Br. no perovskite bandgap tuning, trace yield

When X = CI, bandgap blue-tuning, forming  $CsPbBr_{3-x}CI_x$ , wider photoredox potential, high yield

D) This work: halide-exchange for continous Br radical for photocatalytic [3+2] cycloaddition

Br + h blue LED Br + H
Br 
$$R^2$$
 $R^5$ 
 $R^5$ 
 $R^5$ 
 $R^5$ 
 $R^5$ 
 $R^6$ 
 $R^5$ 
 $R^6$ 
 $R^6$ 

**Scheme 1.** Perovskite-induced Br radical in DBM for photocatalytic [3+2] cycloaddition.

[a] Y. Lin, Prof. Dr. Y. Yan Department of Chemistry and Biochemistry San Diego State University 5500 Campanile Drive, San Diego, CA-92182 (USA) E-mail: yong.yan@sdsu.edu Homepage: https://yan.sdsu.edu/

Supporting information for this article is available on the WWW under https://doi.org/10.1002/cssc.202301060

© 2023 The Authors. ChemSusChem published by Wiley-VCH GmbH. This is an open access article under the terms of the Creative Commons Attribution Non-Commercial License, which permits use, distribution and reproduction in any medium, provided the original work is properly cited and is not used for commercial purposes.

methane forming CsPbBr<sub>3-x</sub>Cl<sub>x</sub> (Scheme 1B), [13] implying a potential application in halogen activations. We also reported a perovskite-induced photocatalytic organic reaction for the synthesis of N-heterocycles, forming a critical pharmaceuticalrelated N-aryl pyrrole scaffold, that involved in-situ lightinduced halide-exchange between α-haloketone and CsPbBr<sub>3</sub>,



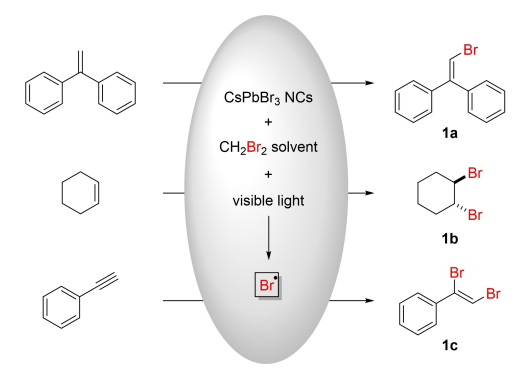
leading to a wider photoredox potential of the perovskite photocatalyst thus enabling a broader range of substrate activation (Scheme 1C). [10a]

Halide-exchange has been focused on tuning the bandgap of halide perovskite, therefore tuning its respective optoelectronic properties. The proposed mechanism for light-induced halide-exchange with organohalides involves a key electron transfer step from excited-state NCs (conduction band) to reduce haloalkane, forming respective halide anion and alkyl radical.[13-14] Fewer attentions have been paid to the halide itself, particularly organohalides, one of the most common organic compounds. Noticeable exception was reported for halogenation of electron-rich arenes where halogen sourced from dihalomethane solvent.[15] Wong et al. illustrated the exchange kinetics using primary, secondary, and tertiary haloalkanes and demonstrated that the exchange rate is determined by the activation barrier of C-X bond breakage, and closely corresponds to the C-X bond energy and respective carbon radical stability.<sup>[14]</sup> However, the hole-transfer counterpart (valance band-based oxidation), which is an imperative half-cell reaction of the full cycle, of such light-induced halide-exchange process has been less discussed.

#### **Results and Discussion**

#### **Bromine radicals**

Our initial exploration of this oxidative half-cell reaction reveals that the photogenerated holes may directly transfer to the halide anions, i.e., Br<sup>-</sup>, that has been generated from the reductive half-cell reaction (electron transfer process), forming Br<sup>•</sup> in DBM solvent as shown in Scheme 1D. We employed reported method to verify such Br<sup>•</sup> intermediate. For instance, when 1,1-diphenylethylene, a commonly known radical acceptor, was added to a DBM solution containing catalytic amount of CsPbBr<sub>3</sub> NCs, a substantial portion of 2-bromo-1,1-diphenylethylene (1a) was found as product after irradiation under blue LED in anaerobic condition (Scheme 2, also see SI). Furthermore, when cyclohexene and phenylacetylene were subjected to the same experimental conditions respectively, their bromo-addition products (1b and 1c) were also isolated. The production of



Scheme 2. Bromine radical trapping.

the bromo-trapping products ( $1\,a$ –c) under CsPbBr $_3$  NCs photocatalysis conditions in DBM underpins the Br $^{\bullet}$  formation from the hole oxidation of the Br $^-$  that are generated from the first electron transfer step.

Interestingly, we also found that such perovskite-induced Br\* generation in DBM is a continuous process under the visible light irradiation. Br\* is known to brominate the reactive C-H bonds, i.e., benzylic C-H, via free-radical substitution. Our experiment of gram-scale benzylic bromination of toluene shows that the yield of benzyl bromide steadily increased over 14 days. (Table S3) This remarkable result further demonstrates two important points: 1) the steady-state concentration of Br\* during the light-induced perovskite bromide-exchange process is low, otherwise multi-bromination byproduct could be seen; 2) Br can be continuously generated without undesirable quenching during the photocatalysis process. The presence of small amount but continuous generation of precious Br\* in such a neat reaction setup might be of significance for further development of valuable photocatalytic reactions, given that Br\* has been widely explored as an agent for bromination, hydrogen atom transfer (HAT)[16,17] and other elegant organic transformations.[18]

#### Photocatalytic design

We focus on exploiting the perovskite-induced continuous Br<sup>o</sup> for photocatalytic organic reaction purposes. Here we explore the synthetic application of this system by designing a protocol for Br radical-mediated [3+2] cycloaddition for vinylcyclopentane synthesis. Five-membered cyclic scaffolds are privileged in medicinal chemistry and being found in over 10 of the top 30 Bemis-Murcko frameworks.<sup>[19]</sup> Several seminal works were reported to achieve [3+2] cycloaddition between vinylcyclopropanes and alkenes. Examples by thiyl radical were found in early cases under thermal condition or with a radical initiator under intense UV excitation. [20] Organotin hydride, a classical radical precursor, was reported to be active towards this endeavor with the presence of a suitable radical initiator. [21] As the rapid development of visible-light photocatalysis, Miyake group reported that a cinnamyl bromide co-catalyst can accept triplet energy from an excited-state iridium photocatalyst to mediate such valuable organic transformation. [22] Most recently, isothiouronyl radical cation coupled with an Ir-based photocatalyst was utilized to catalyze this [3+2] cycloaddition. [23] Overall, the harsh reaction conditions, radical initiator, delicately designed co-catalyst or noble metal complex-based photocatalyst were required for the success of the aforementioned reactions.

Such radical-mediated [3+2] cycloaddition mechanism necessitates a highly reversible addition of the catalytic radical (i.e., Br\*) to the  $C(sp^2)$ – $C(sp^2)$  bond of vinylcyclopropane substrate achieving ring opening and then to release the added radical after a cyclization step. However, the continuous radical generation may be beneficial to the [3+2] product formation because the undesirable but inevitable off-cycle quenching of such radicals will terminate the reaction and

result in a diminished yield.<sup>[25]</sup> Our approach here featuring a benign reaction condition with recyclable CsPbBr<sub>3</sub> NCs as the photocatalyst, DBM as the co-catalyst and solvent, demonstrates a high turnover pathway to exploit the photogenerated holes during the perovskite halide-exchange process. The CsPbBr<sub>3</sub> perovskite-induced continuous Br• generation under visible light irradiation in our simple reaction setup may offer an appealing strategy for photocatalytic Br radical-mediated organic transformations.

#### Reaction development

To our delight, visible-light-induced continuous Br\* generated from CsPbBr<sub>3</sub> NCs in DBM resulted in the [3+2] cycloaddition of vinylcyclopropane 2a with alkene 3a in a high yield as shown in Table 1. The desired product vinylcyclopentane 4a was observed with a diastereomeric ratio (d.r.) of 2:1 (cis/trans) in 94% yield after blue LED irradiation for 4 h (Table 1, entry 1). Omitting the light or NCs resulted in complete recovery of the starting materials (entries 2, 3 and 4), demonstrating the pivotal role of CsPbBr3 NCs as a photocatalyst. Furthermore, non-Br solvent resulted in no reaction (entries 5 and 6) or trace yield (entry 7). Altering the Br-based solvent, ratio between the starting materials 2a and 3a resulted in compromised yields (entries 8, 9 and 10). Note that a stoichiometric instead of solvent amount of DBM could also achieve a similar yield to the optimized conditions, but a longer reaction time was required (see Table S1 for full condition exploration).

**Table 1.** Optimization studies and control experiments for perovskite photocatalytic Br-mediated [3+2] cycloaddition.

CsPbBr<sub>3</sub> NCs

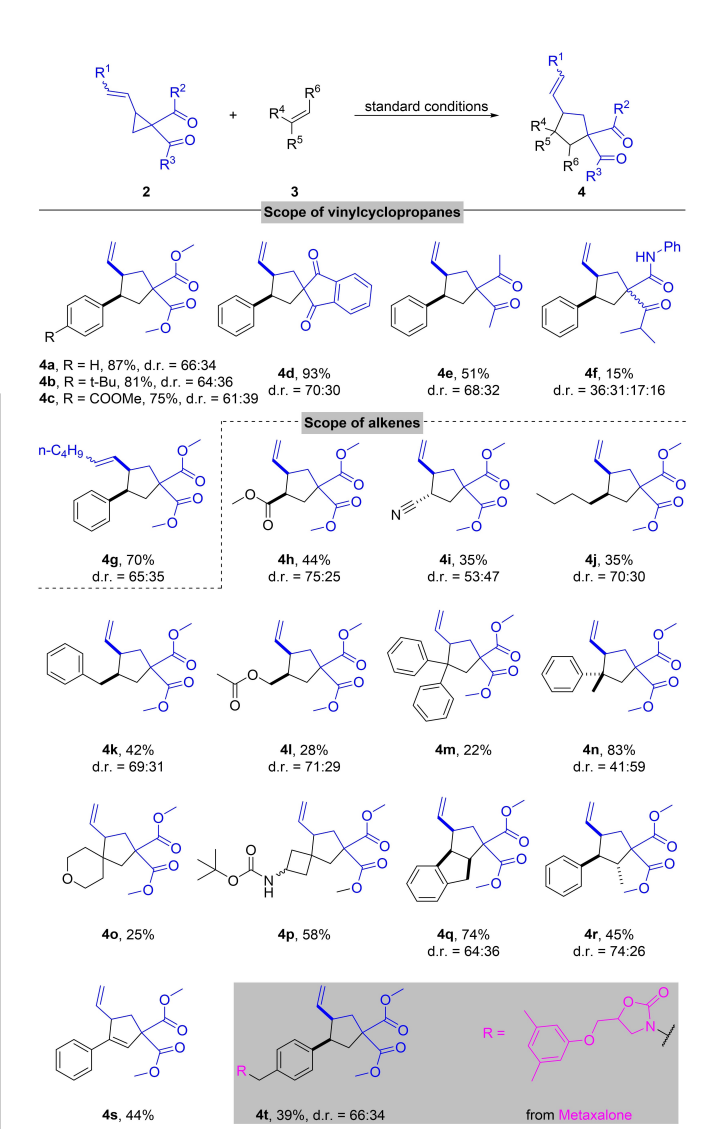
1	None	94 (87)
2	No light	0
3	No CsPbBr <sub>3</sub> NCs	0
4	PbBr <sub>2</sub> instead of CsPbBr <sub>3</sub> NCs	0
5	Toluene as solvent	0
6	Tetrahydrofuran as solvent	0
7	Dichloromethane as solvent	Trace
8	1-Bromobutane as solvent	91
9	<b>3 a</b> (1.0 equiv.)	68
10	<b>3 a</b> (3.0 equiv.)	92

[a] Standard conditions: **2 a** (0.15 mmol, 0.1 M), **3 a** (0.30 mmol, 2.0 equiv.), CsPbBr<sub>3</sub> NCs (1.0 mg), DBM (1.5 mL). Reaction was performed under N<sub>2</sub> and 40 W blue LED ( $\lambda_{\rm max} = 456$  nm) irradiation at room temperature for 4 h. [b] Yields were determined by  $^1\text{H}$  NMR spectroscopy using 3,4,5-trichloropyridine as an internal standard. Isolated yield is shown in parentheses.

## Reaction scope

The reaction scope with regard to both vinylcyclopropanes 2 and alkenes 3 were investigated (Scheme 3). 2 with different substituents cyclized with styrenes in yields up to 93%. Compound 4f was obtained in a noticeable lower yield (15%), probably due to the steric hindrance from the isopropyl group and that the *N*-phenylacetamido group may function as a competitive hole scavenger, having a detrimental effect on the product yielding. [9e] Notably, the double bond on 2 does not need to be terminal (4g, 70% yield).

We next examined the scope of alkenes. In general, styrenes could tolerate both electron-donating and electron-withdrawing para-substituents, making them highly successful reaction partners (**4a-c**, 75–87% yield). Michael acceptors only delivered products in moderate yields (**4h**, i, 35–44% yield), likely because the undesired polymerization reaction competed with the desired reaction pathway. [26] Another

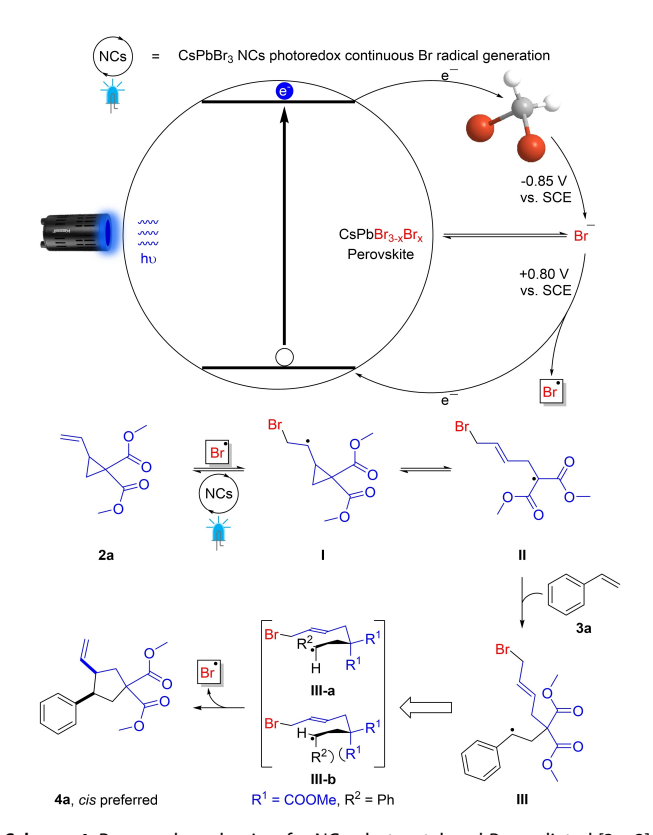


**Scheme 3.** Vinylcyclopropanes and alkenes scope.  $^{[a,b,c]}$  [a] Isolated yields are shown. [b] d.r. values were determined by  $^1H$  NMR. [c] Only the structures of the major diastereomers are shown.

Chemistry Europe

European Chemical Societies Publishing

reason perhaps could be attributed to less-than-optimal matching of orbitals energies, considering an electron-poor malonyl radical (Scheme 4, intermediate II) attacking an electron-deficient alkene. Non-activated primary alkenes are also successful substrates albeit with lower yield (4j-l, 28-42% yield), we attribute such observation to a less stable radical intermediate (Scheme 4, variant of III). (Vide infra) Overall, both Michael acceptors and non-activated primary alkenes delivered products in modest yields. However, the conversions based on starting material 2a were nearly quantitative in these cases. Further analysis on the side products revealed a ring-opening polymerization pathway, consistent to a mechanism disclosed by Chen et al., [27] which consumed the vinylcyclopropane starting material in an unproductive way (Figure S4 and S5). These observations indicate that both the transition from intermediate II to III and the stability of III are imperative for an efficient transformation. Saturated (hetero)cycle compounds with an exomethylene group generated useful three-dimensional-enrich spiro-products (4 o, p, 25-58% yield). Indene, a cyclic alkene, could be employed to generate a fused-ring product (4q, 74% yield) that is an important category in drug discovery. Alpha-methyl substituted styrene did not appear to affect the cycloaddition for 4n, creating a quaternary carbon stereocenter, with a yield of 83% that is comparable to nonsubstituted styrenes. However, beta-methyl substituted styrene delivered product in a lower yield (4r, 45 % yield). As expected, 1,1-diphenylethylene only resulted in 22% yield of



 $\begin{tabular}{ll} Scheme 4. Proposed mechanism for NCs-photocatalyzed Br-mediated [3+2] cycloaddition. \end{tabular}$ 

desired product (4m) with high yielding of 1a as a byproduct, because 1,1-diphenylethylene itself is a good bromine radical acceptor, consuming  $Br^{\bullet}$  during the photocatalytic process as shown in Scheme 2. Interestingly, this [3  $\pm$  2] cycloaddition is not limited to alkenes. Phenylacetylene bearing a triple bond is also a successful substrate to form [3  $\pm$  2] cycloaddition product,  $\pm$  4s. Further studies focusing on the alkyne substrates are currently under investigation in our laboratory. Finally, an alkene derived from the commercially available drug molecule, Metaxalone, provided the expected product (4t) in 39% yield, indicating a potential application in late-stage pharmaceutical functionalization, an extremely important methodology for drug development.

#### Mechanistic investigation

The plausible mechanism (Scheme 4) is premised on our experimental results and previous reported studies. Under visible light irradiation, CsPbBr<sub>3</sub> NCs undergo photoinduced electron transfer from conduction band to DBM ( $E_{p/2}^{ox} = -0.85 \text{ V}$ vs. SCE, [15] also see Supporting Information), generating Br-(Scheme 1D and Scheme 4), while the photogenerated holes from valence band further oxidize the Br<sup>-</sup> into Br<sup>•</sup> ( $E_{p/2}^{red} = +$ 0.80 V vs. SCE).[28] Here, the bromide-exchange between the DBM solvent and CsPbBr<sub>3</sub> NCs is a dynamic process under light irradiation, meaning that Br\* generation is continuous in the photoredox cycle. Note that direct single-electron oxidation of DBM is not viable because the reduction potential of DBM (E<sub>D</sub>/  $_{2}^{\text{red}}$  = +1.62 V vs. SCE)<sup>[16]</sup> is out of reach for the photoredox potential of CsPbBr<sub>3</sub> NCs. The reversible addition of Br\* to vinylcyclopropane 2a leads to intermediate I, followed by ring opening to form II, which is then trapped by alkene 3a to produce III. The optimal reaction condition requires an excessive amount of 3a (Table 1, entry 9), probably because of the reversible nature of intermediate II which resonates with I. But over-excess amount of 3a slightly reduces the yield (Table 1, entry 10), because 3a may compete with 2a for the Br\* addition (such as shown in Scheme 2), therefore consuming Br<sup>•</sup> in an undesirable way.

The diastereoselectivity is governed by the intermediate III, whose chair-like transition states have been proposed in Scheme 4, bracket. [20b] Two likely configurations III-a and III-b are illustrated as the key transition states for the de-brominated (Br regeneration) cyclization step and determine the diastereoselectivity. For instance, III-a will lead to the formation of cis-4a while III-b results in the trans-4a product. Here, the steric hindrance from the 1,3-diaxial interaction of **III-b** (i.e., R<sup>1</sup> and R<sup>2</sup>) disfavors the III-b configuration compared to the III-a that dictates the preference for cis-product formation, corroborating with the general diastereomeric ratios shown in Scheme 3.<sup>[29]</sup> The diastereomeric conformation of the product is confirmed by nuclear overhauser effect spectroscopy (NOESY NMR, see SI). It is worth noting that our illustration of the diastereoselectivity of this transformation is distinct from the lately reported photocatalytic approach. [22,23]



Photocatalyst evaluation studies were carried out employing a few commonly used homogeneous molecular photocatalysts (Table 2). Note that the key to a successful transformation is to efficiently produce continuous Br\* without perturbing the subsequent catalytic cycle. Under otherwise the same standard conditions, Ru(bpy)<sub>3</sub><sup>2+</sup> yielded no product because the redox potential of it cannot reach that of DBM (Table 2, entry 2). Although fac-Ir(ppy)<sub>3</sub> can photoreduce DBM to Br<sup>-</sup> ( $Ir^{IV}/Ir^{III*} = -1.73 \text{ V}$  vs. SCE), it barely reaches the reduction potential of Br<sup>-</sup> to Br<sup>•</sup> ( $Ir^{IV}/Ir^{III} = +0.77 \text{ V vs. SCE}$ ). The key oxidation step to generate Br\* might be impeded, hence only trace amount of product was observed. [Acr-Mes]<sup>+</sup>(ClO<sub>4</sub>)<sup>-</sup> photocatalyst yielded trace amount of desired product owing to its strong excited-state reduction potential  $(cat^*/cat^{\bullet} = +2.06 \text{ V} \text{ vs. SCE})$ , which allows it to directly oxidize the DBM to generate Br\*. However, the Br\* generation is not continuous hence not sustainable because now the other half-cell reaction (reduction) is problematic due to the absence of a proper reagent to regenerate the ground-state acridinium photocatalyst, causing the following Br radicalmediated catalytic cycle susceptible to termination once the limited amount of Br\* being produced is intercepted by an off-cycle pathway. 4-CzIPN photocatalyst furnished a good amount of product, likely going through a reduction (DBM/ Br<sup>-</sup>) then oxidation (Br<sup>-</sup>/Br<sup>•</sup>) mechanism. Since the photoredox potentials of 4-CzIPN (cat $^+$ /cat $^*$  = -1.04 V, cat $^+$ /cat = + 1.52 V vs. SCE) are amendable to cover both the oxidation potential of DBM and the reduction potential of Br<sup>-</sup>. Finally, a Br-containing fluorescein-based PC, eosin Y, with suitable excited-state photoredox potentials was subjected to this study. However, the product was only observed in a low yield even with the presence of CsBr salt as an additive (Table 2, entry 6). The above results further support our photoredoxbased continuous Br\* generation mechanism.

## Catalyst recycling

Our heterogenous approach may be advantageous over homogenous photocatalysts for such [3+2] cycloaddition in the following aspects. 1) The localized concentration of Br<sup>-</sup> is higher in the case of CsPbBr<sub>3</sub> NCs owing to its positivelycharged surface<sup>[31]</sup> hence more capable of adsorbing Br<sup>-[13]</sup> as the potential hole acceptor. 2) The Br may also come from CsPbBr<sub>3</sub>'s own surface, which is supported by our observation (Table 1, entry 7),[32] meaning the NCs are intrinsically superior in the context of bromide oxidation. Note that this pathway is not necessarily detrimental to the perovskite structure since Br diffusing from the bulk solution would compensate for the loss from the NCs' surface. Conversely, the density of surface vacancy defects of CsPbBr<sub>3</sub> NCs could be reduced via such "self-bromide exchange" process. [13] 3) The enhancement of PL intensity of CsPbBr<sub>3</sub> NCs after irradiation in DBM was observed in our study (Figure S6), in line with previous report, [13] indicating the defects healing during the "self-bromide exchange" process. Catalyst deactivation remains a long-term issue.[33] However, our recycling experiments show that the perovskite NCs demonstrated no sign of decrease in catalytic performance during three consecutive cycles of reactions (Table S2), probably attributed to this self-healing process. These aspects together undoubtedly render a high turnover photocatalytic strategy.

#### **More Applications**

We moved on to examine the robustness of our system by merging it with other bromination or Br-mediated reactions. The preliminary results without optimization are very promising. Various alkylbenzene compounds were successfully brominated at the benzylic position in moderate yields (Scheme 5A). Notably, ibuprofen, a commonly used anti-inflammatory drug molecule, derived methyl ester could

Table 2. Photocatalyst (PC) evaluation under standard conditions.								
PC (1.0 mg) DBM solvent (0.1 M) blue LED (\(\lambda_{\text{max}} = 456 \text{ nm}\) N <sub>2</sub> , r.t., 4 h								
		2a (0.15 mmol) 3a (2.0 ed	quiv.)	4a				
Entry	PC	Potential of redox couple [V] <sup>[a]</sup>						
		M+/M*	$M*/M^-$	$M^+/M$	$M/M^-$	[%] <sup>[b]</sup>		
1	CsPbBr <sub>3</sub> NCs	-1.3	+1.1			94		
2	$Ru(bpy)_3^{2+}$	-0.81	+ 0.77	+1.29	-1.33	n.d.		
3	fac-lr(ppy)₃	-1.73	+0.31	+0.77	-2.19	trace		
4	$[Acr ext{-}Mes]^+$ $(ClO_4)^-$		+ 2.06		-0.57	trace		
5	4-CzIPN	-1.04	+ 1.35	+ 1.52	-1.21	68		
6	Eosin Y	-1.11	+0.83	+0.78	-1.06	21 (24)		

[a] All potentials vs. saturated calomel electrode (SCE). Photoredox potentials of PC are from literature. [30] [b] Yields were determined by <sup>1</sup>H NMR using 3,4,5-trichloropyridine as an internal standard. Yield with CsBr (1.0 mg) as an additive is shown in parentheses.

Scheme 5. Merging with other organic transformations. [a,b] [a] Isolated yields are shown. [b] General reaction conditions: substrate (0.15 mmol, 0.1 M),  $CsPbBr_3$  NCs (1.0 mg), DBM (1.5 mL). Reaction was performed under  $N_2$  and 40 W blue LED ( $\lambda_{max}$  = 456 nm) irradiation at room temperature.

undergo bromination to generate 5 c (28 % yield). Gram-scale selective synthesis of an important building block, benzyl bromide, from widely available toluene was performed to demonstrate the scale-up capability of this system. (Table S3) We also discovered that mono-bromomethane was a key side product generated from DBM in this benzylic bromination. A series of electron-rich (hetero)arenes werebrominated at the predictable position (Scheme 5B, 6a-c, 34-56% yield). Gratifyingly, our system could also be applied to an HAT reaction, where the tertiary C(sp³)—H of benzaldehyde acetals can be abstracted by Br<sup>•</sup> then undergo β-fragmentation to produce respective esters (Scheme 5C). This type of mechanism was well-documented by Doyle Group<sup>[17c,34]</sup> (also see SI). More synthetic applications utilizing this strategy are currently under development in our group.

### Conclusions

Mechanistic investigation of visible-light-induced halide-exchange between lead-halide perovskite NCs and organohalide solvents leads to the discovery of an important Br\* intermediate. Such Br\* is concluded to be generated in a continuous manner in DBM solvent under visible light irradiation. We also prove that such continuous generation of Br\* plays an important role in further design of photocatalytic organic reactions. Most prominently, such mechanism allows us to utilize DBM as a cocatalyst and solvent to mediate the perovskite-induced [3+2] cycloadditions with broad substrate scope tolerance, for the synthesis of a critical category in medicinal chemistry. The respective diastereoselectivity for the preference of cis-product formation has been revealed due to the 1,3-diaxial interaction of the chair-like transition states (III-a vs. III-b). Additionally, this strategy can be extended to other Br radical-related reactions, i.e., benzylic bromination, aromatic bromination, and Br radicalmediated HAT, demonstrating a great potential for halide perovskite to be applied in halogen radical-involved organic

Among the photocatalysts for photoredox organic synthesis, halide perovskites are not only economic but also highly efficient, paving the path to render the ease of product separation, simple catalyst regeneration, and usually high stability of solid catalysts facilitating continuous flow production processes. The design and development of heterogeneous catalysts for vast and large-scale production of value-added organic molecules, particularly those of pharmaceutical significance, i.e., [3+2] cycles here, should be an essential ingredient in the chemical synthetic toolbox.

## **Experimental Section**

Preparation of CsPbBr<sub>3</sub> NCs photocatalyst. The synthesis of CsPbBr<sub>3</sub> perovskite nanocrystals was adapted from literature. [35] CsBr solution (3.0 mL, 1.0 M in H<sub>2</sub>O) and PbBr<sub>2</sub> solution (7.0 mL, 1.0 M in dimethylformamide, DMF) were prepared as two respective precursor stock solutions. To a 20-mL vial with a magnetic stirring bar, hexanes (10.0 mL) and oleic acid (2.0 mL) were added and the resulting mixture was allowed to vigorously stir at room temperature for 5 min. Then, n-octylamine (0.25 mL) was added and continued stirring for another 5 min. Next, the PbBr $_2$  stock solution (300  $\mu$ L, 1.0 M in DMF) was added dropwise. After 5 min stirring, the CsBr stock solution (300 μL, 1.0 M in H<sub>2</sub>O) was added dropwise. The resulting mixture was allowed to stir for another 5 min followed by adding acetone (8.0 mL) in one batch. A large amount of precipitate was formed and the mixture stayed stirring for 1 min and was subjected to vortex for 30s. Finally, the solid was collected via centrifugation and washed with MeOAc (3 mL). The residual solvent was removed by vacuum oven at 50°C for 2 h.

General procedure for the synthesis of vinylcyclopropanes. The synthesis of substrate 2 was adapted from literature. [36] To a roundbottom flask with a magnetic stirring bar was added 1,4-dibromo-2butene (1.0 equiv.), K<sub>2</sub>CO<sub>3</sub> (3.0 equiv.), acetone (0.33 M) and 1,3dione (1.0 equiv.). The resulting mixture was allowed to react at reflux temperature around 60°C for 24 h. Upon completion, the reaction mixture was filtered and the solvent was removed by rotary evaporator. Then the product was purified by flash column chromatography on silica gel using a combination of hexanes and EtOAc as eluent. TLC was employed to detect the product and the basic KMnO<sub>4</sub> solution was necessary in most of the cases for visualization in addition to UV lamp (254 nm).

General procedure for the [3+2] cycloaddition. To a 1-dram vial with a magnetic stirring bar was added vinylcyclopropane 2 (0.15 mmol, 1.0 equiv.), DBM (1.5 mL, 0.1 M), CsPbBr<sub>3</sub> perovskite photocatalyst (1.0 mg) and alkene 3 (0.30 mmol, 2.0 equiv.). The resulting mixture was degassed with N<sub>2</sub> for 20 min and sealed with parafilm. It was allowed to react at room temperature under blue LED (Kessil, 40 W,  $\lambda_{max}$  = 456 nm) irradiation for 4 h. Upon completion, the solvent was removed by rotary evaporator. Then the product 4 was purified by flash column chromatography on silica gel using a combination of hexanes and EtOAc as eluent. TLC was employed to detect the product and the basic KMnO<sub>4</sub> solution was necessary in most of the cases for visualization in addition to UV lamp (254 nm).



## **Supporting Information**

The authors have cited additional references within the Supporting Information. [17c,22, 27, 34–37]

# **Acknowledgements**

The photocatalytic organic synthesis exploration is supported by NSF CAREER award (CHE-2140261) to Y.Y. The hybrid materials design and development are supported as part of the Center of Hybrid Organic Inorganic Semiconductors for Energy (CHOISE) an Energy Frontier Research Center funded by the Office of Science, Office of Basic Energy Sciences within the US Department of Energy.

## **Conflict of Interests**

The authors declare no conflict of interest.

# **Data Availability Statement**

The data that support the findings of this study are available in the supplementary material of this article.

**Keywords:** bromine radicals  $\cdot$  perovskites  $\cdot$  [3+2] cycloaddition  $\cdot$  heterogeneous photocatalysis  $\cdot$  photoredox

- [1] a) J. Y. Kim, J.-W. Lee, H. S. Jung, H. Shin, N.-G. Park, Chem. Rev. 2020, 120, 7867–7918;
   b) J.-P. Correa-Baena, M. Saliba, T. Buonassisi, M. Grätzel, A. Abate, W. Tress, A. Hagfeldt, Science 2017, 358, 739–744.
- [2] a) Y. Guo, C. Liu, H. Tanaka, E. Nakamura, J. Phys. Chem. Lett. 2015, 6, 535–539; b) L. Dou, Y. M. Yang, J. You, Z. Hong, W. H. Chang, G. Li, Y. Yang, Nat. Commun. 2014, 5, 5404.
- [3] Z.-K. Tan, R. S. Moghaddam, M. L. Lai, P. Docampo, R. Higler, F. Deschler, M. Price, A. Sadhanala, L. M. Pazos, D. Credgington, F. Hanusch, T. Bein, H. J. Snaith, R. H. Friend, *Nat. Nanotechnol.* 2014, 9, 687–692.
- [4] H. Zhu, Y. Fu, F. Meng, X. Wu, Z. Gong, Q. Ding, M. V. Gustafsson, M. T. Trinh, S. Jin, X. Y. Zhu, Nat. Mater. 2015, 14, 636–642.
- [5] T. C. Sum, N. Mathews, G. Xing, S. S. Lim, W. K. Chong, D. Giovanni, H. A. Dewi, Acc. Chem. Res. 2016, 49, 294–302.
- [6] Y.-M. You, W.-Q. Liao, D. Zhao, H.-Y. Ye, Y. Zhang, Q. Zhou, X. Niu, J. Wang, P.-F. Li, D.-W. Fu, Z. Wang, S. Gao, K. Yang, J.-M. Liu, J. Li, Y. Yan, R.-G. Xiong, *Science* 2017, 357, 306–309.
- [7] J. S. Manser, J. A. Christians, P. V. Kamat, Chem. Rev. 2016, 116, 12956– 13008.
- [8] a) S. Shyamal, N. Pradhan, J. Phys. Chem. Lett. 2020, 11, 6921–6934;
  b) K. S. Schanze, P. V. Kamat, P. Yang, J. Bisquert, ACS Energy Lett. 2020,
  5, 2602–2604; c) C. Han, X. Zhu, J. S. Martin, Y. Lin, S. Spears, Y. Yan, ChemSusChem 2020, 13, 4005–4025.
- [9] a) J. S. Martin, X. Zeng, X. Chen, C. Miller, C. Han, Y. Lin, N. Yamamoto, X. Wang, S. Yazdi, Y. Yan, M. C. Beard, Y. Yan, J. Am. Chem. Soc. 2021, 143, 11361–11369; b) Y. Lin, J. Guo, J. San Martin, C. Han, R. Martinez, Y. Yan, Chem. Eur. J. 2020, 26, 13118–13136; c) X. Zhu, Y. Lin, Y. Sun, M. C. Beard, Y. Yan, J. Am. Chem. Soc. 2019, 141, 733–738; d) H. Lu, X. Zhu, C. Miller, J. San Martin, X. Chen, E. M. Miller, Y. Yan, M. C. Beard, J. Chem. Phys. 2019, 151, 204305; e) Y. Lin, M. Avvacumova, R. Zhao, X. Chen, M. C. Beard, Y. Yan, ACS Appl. Mater. Interfaces 2022, 14, 25357–25365.
- [10] a) X. Zhu, Y. Lin, J. San Martin, Y. Sun, D. Zhu, Y. Yan, Nat. Commun. 2019, 10, 2843; b) Y.-F. Si, K. Sun, X.-L. Chen, X.-Y. Fu, Y. Liu, F.-L. Zeng, T. Shi, L.-B. Qu, B. Yu, Org. Lett. 2020, 22, 6960–6965; c) A. Shi, K. Sun, X. Chen, L. Qu, Y. Zhao, B. Yu, Org. Lett. 2022, 24, 299–303; d) B. Pal, A.

- Mathuri, A. Manna, P. Mal, *Org. Lett.* **2023**, *25*, 4075–4079; e) K. Mishra, D. Guyon, J. San Martin, Y. Yan, *J. Am. Chem. Soc.* **2023**, *145*, 17242–17252.
- [11] T. Shi, K. Sun, X.-L. Chen, Z.-X. Zhang, X.-Q. Huang, Y.-Y. Peng, L.-B. Qu, B. Yu, Adv. Synth. Catal. 2020, 362, 2143–2149.
- [12] a) Q. A. Akkerman, V. D'Innocenzo, S. Accornero, A. Scarpellini, A. Petrozza, M. Prato, L. Manna, J. Am. Chem. Soc. 2015, 137, 10276–10281;
  b) D. M. Jang, K. Park, D. H. Kim, J. Park, F. Shojaei, H. S. Kang, J.-P. Ahn, J. W. Lee, J. K. Song, Nano Lett. 2015, 15, 5191–5199;
  c) G. Nedelcu, L. Protesescu, S. Yakunin, M. I. Bodnarchuk, M. J. Grotevent, M. V. Kovalenko, Nano Lett. 2015, 15, 5635–5640.
- [13] D. Parobek, Y. Dong, T. Qiao, D. Rossi, D. H. Son, J. Am. Chem. Soc. 2017, 139, 4358–4361.
- [14] Y.-C. Wong, W.-B. Wu, T. Wang, J. D. A. Ng, K. H. Khoo, J. Wu, Z.-K. Tan, Adv. Mater. 2019, 31, 1901247.
- [15] Y. Li, T. Wang, Y. Wang, Z. Deng, L. Zhang, A. Zhu, Y. Huang, C. Zhang, M. Yuan, W. Xie, ACS Catal. 2022, 12, 5903–5910.
- [16] P. Jia, Q. Li, W. C. Poh, H. Jiang, H. Liu, H. Deng, J. Wu, Chem 2020, 6, 1766–1776.
- [17] a) H. Wang, H. Liu, M. Wang, M. Huang, X. Shi, T. Wang, X. Cong, J. Yan, J. Wu, iScience 2021, 24, 102693; b) J. M. Tanko, M. Sadeghipour, Angew. Chem. Int. Ed. 1999, 38, 159–161; c) S. Dongbang, A. G. Doyle, J. Am. Chem. Soc. 2022, 144, 20067–20077.
- [18] a) I. Saikia, A. J. Borah, P. Phukan, Chem. Rev. 2016, 116, 6837–7042; b) T. Kippo, K. Hamaoka, I. Ryu, J. Am. Chem. Soc. 2013, 135, 632–635.
- [19] G. W. Bemis, M. A. Murcko, J. Med. Chem. 1996, 39, 2887–2893.
- [20] a) K. Miura, K. Fugami, K. Oshima, K. Utimoto, *Tetrahedron Lett.* **1988**, *29*, 5135–5138; b) K. S. Feldman, H. M. Berven, P. H. Weinreb, *J. Am. Chem. Soc.* **1993**, *115*, 11364–11369; c) T. Hashimoto, Y. Kawamata, K. Maruoka, *Nat. Chem.* **2014**, *6*, 702–705.
- [21] H. Zhang, D. P. Curran, J. Am. Chem. Soc. 2011, 133, 10376–10378.
- [22] D.-F. Chen, C. H. Chrisman, G. M. Miyake, ACS Catal. 2020, 10, 2609– 2614.
- [23] G. Archer, P. Cavalère, M. Médebielle, J. Merad, Angew. Chem. Int. Ed. 2022, 61, e202205596.
- [24] A. Studer, D. P. Curran, Angew. Chem. Int. Ed. 2016, 55, 58–102.
- [25] M. A. Cismesia, T. P. Yoon, Chem. Sci. 2015, 6, 5426-5434.
- [26] Y.-C. Wong, J. De Andrew Ng, Z.-K. Tan, Adv. Mater. 2018, 30, 1800774.
- [27] D.-F. Chen, B. M. Boyle, B. G. McCarthy, C.-H. Lim, G. M. Miyake, J. Am. Chem. Soc. 2019, 141, 13268–13277.
- [28] P. Zhang, C. C. Le, D. W. C. MacMillan, J. Am. Chem. Soc. 2016, 138, 8084–8087.
- [29] This transformation favors a conformation that can minimize the 1,3-diaxial interaction in the chair-like transition state III-a/b. The bulkiness of a carbon-centered substituent generally follows the trend:  $C(sp^3) > C(sp^2) > C(sp)$ . For compound 4n, since the methyl is bulkier than the phenyl group, the compound favors a *trans*-conformation where the methyl and the vinyl group are on the same side. For compound 4i, since the nitrile group (sp hybridization) is linear, the 1,3-diaxial interaction is weak, hence the *d.r.* value of it is nearly 1:1.
- [30] a) V. K. Ravi, G. B. Markad, A. Nag, ACS Energy Lett. 2016, 1, 665–671;
  b) C. K. Prier, D. A. Rankic, D. W. C. MacMillan, Chem. Rev. 2013, 113, 5322–5363;
  c) N. A. Romero, D. A. Nicewicz, Chem. Rev. 2016, 116, 10075–10166;
  d) H. Uoyama, K. Goushi, K. Shizu, H. Nomura, C. Adachi, Nature 2012, 492, 234–238;
  e) M. Neumann, S. Füldner, B. König, K. Zeitler, Angew. Chem. Int. Ed. 2011, 50, 951–954.
- [31] a) S. Wei, Y. Yang, X. Kang, L. Wang, L. Huang, D. Pan, Chem. Commun. 2016, 52, 7265–7268; b) S. ten Brinck, I. Infante, ACS Energy Lett. 2016, 1, 1266–1272.
- [32] The CsPbBr<sub>3</sub> NCs first reduce the DCM solvent  $(E_{p/2}^{ox} = -1.04 \text{ V vs. SCE})$  to the respective chloromethyl radical and Cl<sup>-</sup>, then oxidize the Br<sup>-</sup> from its own surface to Br<sup>\*</sup>. Meanwhile, the Cl<sup>-</sup> compensates for the loss of Br<sup>-</sup> from the NCs, transitioning towards CsPbCl<sub>3</sub>. However, since the Br<sup>\*</sup> generation here is very minimum and is not sustainable, only a trace amount of [3+2] cycloaddition product was detected. The Br in this case can only come from the NCs itself.
- [33] M. D. Argyle, C. H. Bartholomew, *Catalysts* **2015**, *5*, 145–269.
- [34] S. K. Kariofillis, S. Jiang, A. M. Żurański, S. S. Gandhi, J. I. Martinez Alvarado, A. G. Doyle, J. Am. Chem. Soc. 2022, 144, 1045–1055.
- [35] H. Huang, F. Zhao, L. Liu, F. Zhang, X.-g. Wu, L. Shi, B. Zou, Q. Pei, H. Zhong, ACS Appl. Mater. Interfaces 2015, 7, 28128–28133.
- [36] R. K. Bowman, J. S. Johnson, *Org. Lett.* **2006**, *8*, 573–576.
- [37] a) F. Wei, C.-L. Ren, D. Wang, L. Liu, Chem. Eur. J. 2015, 21, 2335–2338;
  b) D. Wang, F.-R. Cao, G. Lu, J. Ren, B.-B. Zeng, Tetrahedron 2021, 92, 132250;
  c) M. Kotke, P. R. Schreiner, Tetrahedron 2006, 62, 434–439;



d) A. R. Bogdan, S. L. Poe, D. C. Kubis, S. J. Broadwater, D. T. McQuade, Angew. Chem. Int. Ed. 2009, 48, 8547–8550; e) B. M. Rosen, C. Huang, V. Percec, Org. Lett. 2008, 10, 2597–2600; f) D. Canestrari, C. Cioffi, I. Biancofiore, S. Lancianesi, L. Ghisu, M. Ruether, J. O'Brien, M. F. A. Adamo, H. Ibrahim, Chem. Sci. 2019, 10, 9042–9050; g) K. L. Wilson, J. Murray, C. Jamieson, A. J. B. Watson, Synlett 2018, 29, 650–654; h) S. Song, X. Sun, X. Li, Y. Yuan, N. Jiao, Org. Lett. 2015, 17, 2886–2889; i) F. Bellesia, F. Ghelfi, R. Grandi, U. M. Pagnoni, A. Pinetti, J. Heterocycl. Chem. 1993, 30, 617–621; j) G. A. Molander, L. N. Cavalcanti, J. Org. Chem. 2011, 76, 7195–7203; k) Y. Feng, H. Luo, W. Zheng, S. Matsunaga, L. Lin, ACS Catal. 2022, 12, 11089–11096; l) Q. Liu, G. Li, J. He, J. Liu, P. Li, A. Lei, Angew. Chem. Int. Ed. 2010, 49, 3371–3374; m) X. Song, S. Meng,

H. Zhang, Y. Jiang, A. S. C. Chan, Y. Zou, *Chem. Commun.* **2021**, *57*, 13385–13388; n) I. Ryu, H. Matsubara, S. Yasuda, H. Nakamura, D. P. Curran, *J. Am. Chem. Soc.* **2002**, *124*, 12946–12947; o) M.-L. Yao, M. S. Reddy, L. Yong, I. Walfish, D. W. Blevins, G. W. Kabalka, *Org. Lett.* **2010**, *12*, 700–703.

Manuscript received: July 20, 2023 Revised manuscript received: August 20, 2023 Accepted manuscript online: August 22, 2023 Version of record online: October 26, 2023